

The Trace Element Distribution Patterns of Ediacaran-Early Cambrian Black Shales and the Origin of Selenium in the Guangning Area, Western Guangdong Province, South China

TIAN Xinglei^{1, 2}, LUO Kunli^{1,*} and Andrew V. ZUZA³

¹ Institute of Geographic Sciences and Natural Resources Research, Chinese Academy of Sciences, Beijing 100101, China

² University of the Chinese Academy of Sciences, Beijing 100049, China

³ Nevada Bureau of Mines and Geology, University of Nevada, Reno, Nevada 89557, USA

Abstract: The Ediacaran and early Cambrian black shales are widespread across the South China Craton (Yangtze and Cathaysia blocks). However, the trace element distribution patterns of the Ediacaran and early Cambrian black shales in the Cathaysia Block are still unclear. In this study, thirty-four black shale samples in the Lechangxia Group (Ediacaran) and thirteen black shale samples in the lower Bacun Group (early Cambrian) from Guangning area, western Guangdong Province, South China, were analyzed for major and trace elements concentrations. Compared to the upper continental crust, the Ediacaran black shales exhibit strongly enriched Se, Ga, and As with enrichment factor values (EF) higher than 10, significantly enriched Bi and Rb ($10 > EF > 5$), weakly enriched Mo, Ba, Cs, V, In, Be, Tl, and Th ($5 > EF > 2$), normal U, Cr, Cd, Sc, Pb, Cu, and Li ($2 > EF > 0.5$), and depleted Ni, Zn, Sr, and Co. Early Cambrian black shales display strongly enriched Se, Ga, and As, significantly enriched Ba, Bi, and Rb, weakly enriched Mo, Cs, Cd, V, U, Be, In, and Tl, normal Sc, Th, Cr, Li, Cu, Ni, and Pb and depleted Co, Zn, and Sr. Moreover, Se is the most enriched trace element in the Ediacaran and early Cambrian black shales: concentrations vary from 0.25 to 30.09 ppm and 0.54 to 5.01 ppm, and averaging 4.84 and 1.72 ppm, with average EF values of 96.87 and 34.32, for the Ediacaran and early Cambrian shales respectively. The average concentration of Se in the Ediacaran black shales is 2.8 times higher than that of early Cambrian black shales. Se contents in the Ediacaran and early Cambrian black shales exhibit significant variation ($P = 0.03$). Provenance analysis showed that Se contents of both the Ediacaran and early Cambrian black shales were without detrital provenance and volcanoclastic sources, but of hydrothermal origin. The deep sources of Se and the presence of pyrite may explain the higher Se contents in the Ediacaran black shales. Similar with the Se-rich characteristics of the contemporaneous black shales in the south Qingling Mountain and Yangtze block, the Ediacaran and early Cambrian black shales in Guangning area, Cathaysia, are also enriched in Se, which may provide a clue for looking for the selenium-rich resources in western Guangdong Province.

Key words: black shale, selenium, Ediacaran and early Cambrian, Guangning area, Cathaysia block

1 Introduction

The Ediacaran and early Cambrian are two crucial periods in Earth's history (Knoll and Carroll, 1999; Shen et al., 2010). They witnessed the breakup of the Rodinia supercontinent and the assembly of Gondwanaland (Li et al., 2008; Zhao and Cawood, 2012), oxidation of the ocean-atmosphere system (Fike, 2006; Scott et al., 2008; Sahoo

et al., 2012; Chen et al., 2015), and diversification of early metazoans and “Cambrian Explosion” (Conway Morris, 2000; Knoll et al., 2004; Fike, 2006; Shen et al., 2010; Zhang Xingliang and Shu Degan, 2014).

The South China Craton, which consists of the Cathaysia and Yangtze blocks (Fig. 1a), is one of the largest Precambrian cratons in eastern Asia (Zhao and Cawood, 2012; Li et al., 2014). Black shales, often regarded as “multi-element bearing deposit” (Fan Delian

* Corresponding author. E-mail: luokl@igsnrr.ac.cn

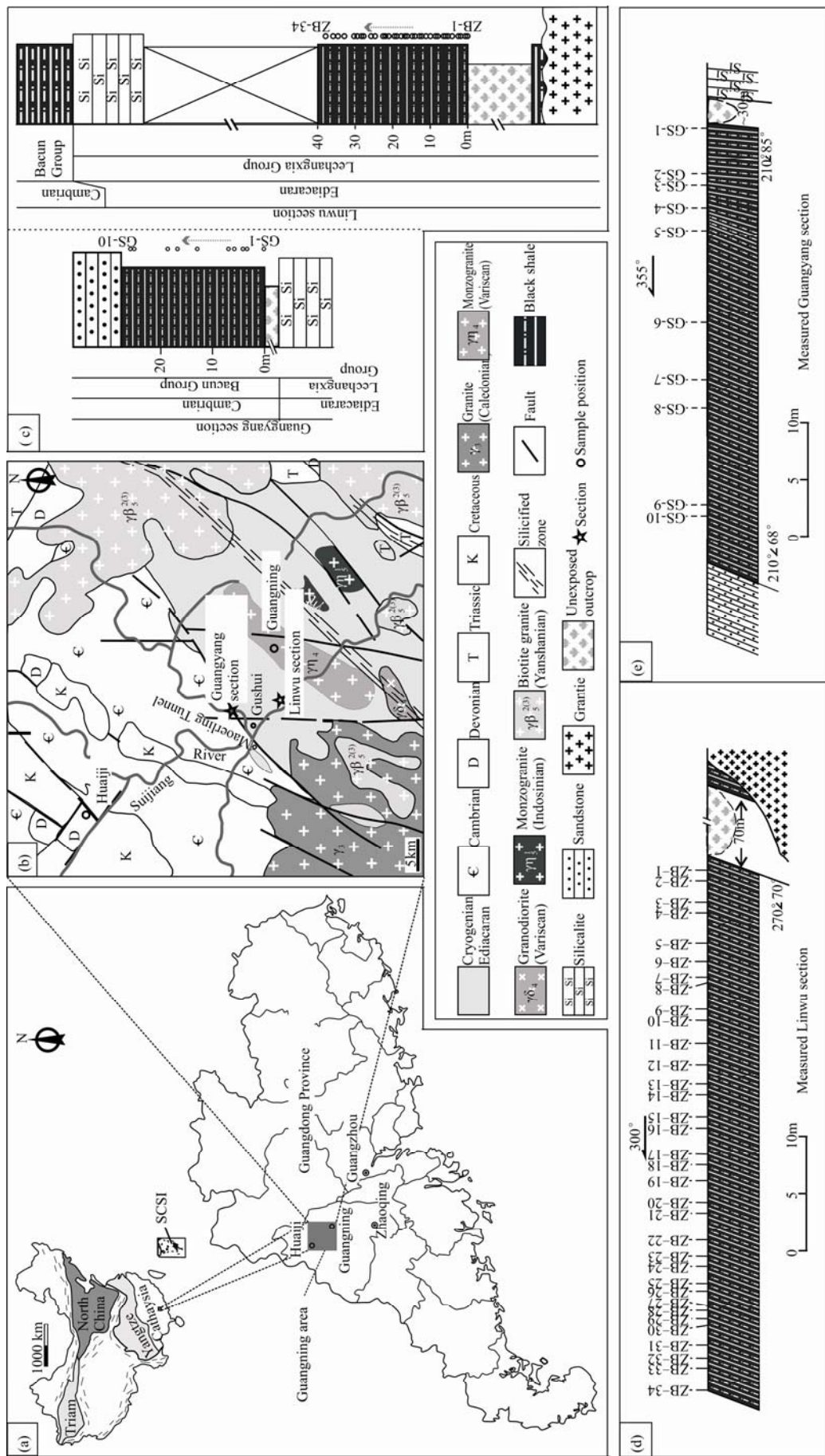


Fig. 1. (a), Tectonic map of the Yangtze platform and Cathaysia; (b), simplified geological map of the Guangning area (after Ma Li'fang., 2002); (c), lithological profiles of the two sections with rock samples taken by this study (marked by black circles); and (d, e), the measured section of Linwu (d) and Guangyang (e).

et al., 1973), always exhibit enriched metallic elements (e.g., platinum family elements, V, U, Mo, Cu, Co, Au, Ag, and Pt), metalloid elements (e.g., As and Se), and rare earth elements (REEs). Widespread thick black shales deposit during the Ediacaran and early Cambrian period in the South China Craton, which represents multi-episodic oceanic anoxic events (Wu Chaodong et al., 1999; Steiner et al., 2001; Scott et al., 2008). Decades of intense geochemical research have already been conducted on the Ediacaran and the early Cambrian black shales in the Yangtze block (Zhuang Hanping et al., 1998; Li Renwei et al., 1999; Zhang Qiuying, 2000; Feng et al., 2004; Feng et al., 2012; Cheng Lixue et al., 2013; Wang Libo et al., 2013; Yu Lingang et al., 2014; Xia Wei et al., 2015). However, little geochemical work has been done on the contemporaneous black shales of the Cathaysia Block. This study is focused on the trace element distribution patterns of the Ediacaran and early Cambrian black shales in the Cathaysia Block.

The average content of selenium (Se) in the upper continental crust is only 0.05 ppm (Taylor and McLennan, 1985; McLennan, 2001). However, the Ediacaran and early Cambrian black shales in the south Qingling Mountain and Yangtze block show Se enrichment (Li Shuangying, 1994; Wen and Qiu, 2002; Feng et al., 2004; Fan et al., 2011), possibly due to hydrothermal fluid, deep source, and/or volcanic influence (Wen and Qiu, 2002; Fan et al., 2011; Feng et al., 2012). Furthermore, the Se-enriched black shales can affect the modern environment. It has been reported that the Se-rich early Cambrian and Ediacaran black rock series (including black shales) are the primary source of the seleniferous environment in Taoyuan Country, Hunan Province of South China (Ni et al., 2015). Additionally, Luo et al. (2004) reported that the sources of extremely high-Se soil in selenosis area at southern Shaanxi Province resulted from the weathering of the local Ediacaran and early Cambrian high-Se strata. Thus, the research for the trace element distribution patterns in the Ediacaran and early Cambrian black shales is particularly necessary to evaluate Se in the modern environment.

The Guangning area (Fig. 1a) in western Guangdong Province has a subtropical monsoon climate and vegetation is well-developed (Qiu Zhihua et al., 2011). The biological and physical weathering of the rocks is intense. However, new artificially-exposed outcrops provide an unsurpassed opportunity to collect the fresh Ediacaran and early Cambrian black shales of the Cathaysia Block. Additionally, chronostratigraphical research has been made in this area (Zhang Zhilan et al., 1992).

In this study, we analyzed the major and trace element

contents of the Ediacaran and early Cambrian black shales collected from Guangning area and documented their distribution patterns to discuss the origin of the selenium.

2 Geological Setting and Samples

The 2750 m thick Lechangxia Group is a flysch deposit that conformably overlies the Yingyangguan Group with a basal pebbly sandstone. The Lechangxia Group underlies the carbonaceous shale of the Cambrian Bacun Group (BGMRGD, 1988; Peng Shaomei et al., 1991; Zhang Zhilan et al., 1992). The pebbly sandstone of Yingyangguan Group has been correlated with the glacial diamictite of Nantuo Formation in the Yangtze block (BGMRGD, 1988; Zhang Zhilan et al., 1992). The upper part of Lechangxia Group contains an algae-rich horizon with *Protoliosphaeridium-Zonoidium* assemblages, which is similar to the Ediacaran Dengying (551–541 Ma) and Doushantuo Formations (635–551 Ma) (Condon et al., 2005) in the Yangtze block of South China (Zhang Zhilan et al., 1992). The lower age bound of the Lechangxia Group is constrained by Pb-Pb detrital zircon age of 995 ± 9 Ma from a tuffaceous siltstone (Zhang Zhilan et al., 1992). Zhang et al. (1992) presented the respective ages of 535 Ma and 556 Ma of the lower part (carbonaceous slate) and the bottom (siliceous-carbonaceous slate) of the Bacun Group and 612 ± 3 Ma of the top part (siliceous layer) of Lechangxia Group by the Pb-Pb whole rock isochron method. In the Guangning area, study area, the Lechangxia Group is ca. 4299 m-thick with more silicalite and carbonaceous shale (BGMRGD, 1988; Zhang Zhilan et al., 1992).

Two sections were measured in this study. The Linwu section ($N23^{\circ}38.077'$; $E112^{\circ}20.699'$) is located beside Linwu village (Fig. 1b), 7 km to the southeast of the town of Gushui. Fresh black shales of the Lechangxia Group are well exposed in a newly excavated surface at the north side of Linwu village (Fig. 1b). Based on the regional stratigraphic sequences, we confirm that the ages of the black shales in Linwu section are older than 612 ± 3 Ma (Zhang Zhilan et al., 1992), which could correlate with the lower part of Ediacaran Doushantuo Formation in Yangtze Gorges area. A total of 34 black shale samples were collected over stratigraphic intervals ranging from 0.54 m to 2.53 m (Fig. 1c and d). The Guangyang section is located beside the Guangyang Hydroelectric Power Station in the town of Gushui ($N23^{\circ}43.460'$; $E112^{\circ}20.215'$) (Fig. 1b) and ten black shales were collected from the outcrop along an unsurfaced road (Figs. 1c and e). The bottom portion (ca. 20 m) of early Cambrian strata as covered, and thus no samples were collected from this section. In addition, other three artificially-exposed fresh

black shales were randomly collected, which were excavated when the new Maoerling Tunnel opened ($N23^{\circ}40.052'$; $E112^{\circ}15.437'$) (Fig. 1b). These three black shales overlie the limestone of the late Ediacaran and could be ensured that they belong to early Cambrian of Bacun Group.

3 Analytical Methods

3.1 Analytical methods

Prior to chemical analyses, the oxide surface of the black shale sample was stripped and fresh parts were chipped and pulverized into powder (less than 200 mesh) for analyses of major, trace and rare earth elements (REE). All samples were analyzed at Laboratory of Analytical and Testing Center (LATC) of the Institute of Geographic Sciences and Natural Resources Research (IGSNRR), Chinese Academy of Sciences (CAS), Beijing, China.

3.1.1 Major and trace elements analysis

Fifty milligrams of powder sample was digested with HNO_3 -HF-HClO₄ using an electric hot plate at $180 \pm 10^{\circ}C$ in a 100-ml PTFE-beaker with a PTFE-beaker cover (Luo, 2011; Tian et al., 2017a; Tian Xinglei and Luo Kunli, 2017b). The PTFE beakers were cleaned for 0.5 h using 20% HNO_3 (v/v) heated to $100^{\circ}C$ in advance. Major, trace and rare earth element concentrations were measured using an Elan DRC-e Inductively Coupled Plasma Optical Emission Spectrometer (ICP-OES) and Perkin-Elmer Optima 5300DV Inductively Coupled Plasma Mass Spectrometry (ICP-MS).

3.1.2 As and Se analysis

Fifty milligrams of powdered sample was used for Se and As analyses. Analytical details are described by Ni et al. (2015). Se and As concentrations were determined by Hydride Generation Atomic Fluorescence Spectrometry (HG-AFS9780; Beijing Haiguang Instruments Co. Ltd).

3.1.3 Loss on ignition (LOI) analysis

A clean porcelain-crucible was placed in a muffle furnace and heated to $900^{\circ}C$ for 30 minutes. The porcelain crucible was removed from the furnace when the temperature fell to $500^{\circ}C$, and was quickly placed in a desiccator. After 10-20 minutes, the weight of the porcelain crucible (m_1) was measured. 1.0 g of powdered sample (m_2) was put in the known-weight of porcelain-crucible and the heating process was repeated as described above. The weight of the heated sample was measured (m_3). The calculated LOI values are as follows: LOI (%) = $\{(m_1 + m_2) - m_3\}/m_2 \times 100$.

3.2 Quality control

Standard samples were prepared identically to the unknowns. Four standards (soil standards GBW07401, GBW07403, and GBW07406, and rock standard GBW 07112 from the Chinese Standard Sample Study Center, Chinese Academy of Measurement Sciences) were used to calibrate element concentrations of the measured samples. Parallel samples, blank experiment and repeated measurements were also used. RSD is commonly better than 10% for both major and trace elements.

4 Results and Discussions

Major and trace elements contents of the samples are given in Table 1-3. An enrichment factor (EF) was calculated as mean elemental concentration/upper continental crust (UCC) according to McLennan (2001). The ratios of Eu/Eu^{*} were calculated by using published formulae from Bau and Dulski (1996), Eu/Eu^{*} = $2Eu_N/(Sm_N + Gd_N)$, and the subscript N in the equation represents the Post-Archean Australian Shale (PAAS) normalized value of the element, and the data for PAAS are from Nance and Taylor (1976). Percentage composition of SiO₂ was estimated as follows: SiO₂(%) = $100 - LOI(\%) - (Al_2O_3 + CaO + Fe_2O_3 + K_2O + Na_2O + MgO + MnO + P_2O_5 + TiO_2)(\%)$.

4.1 Major element oxides

Compared to average values for PAAS (Taylor and McLennan, 1985; McLennan, 2001), Ediacaran black shales contain a slightly higher content of K₂O and SiO₂, and lower proportions of other major element oxides (Table 4). Early Cambrian black shales exhibit a slightly higher content of K₂O, Al₂O₃, and SiO₂, while lower proportions of other major element oxides relative to average values for PAAS (Table 4) (Taylor and McLennan, 1985; McLennan, 2001).

4.2 Trace elements

According to their degree of enrichment, the elements in the samples can be divided into five categories: strongly enriched (EF>10), significantly enriched (10>EF>5), weakly enriched (5>EF>2), normal (2>EF>0.5), and depleted (0.5>EF).

Se, Ga, and As are strongly enriched in the Ediacaran black shales, Bi and Rb are significantly enriched, Mo, Ba, Cs, V, In, Be, Tl, and Th are weakly enriched, and U, Cr, Cd, Sc, Pb, Cu, and Li are close to the average values for UCC (2>EF>0.5) (Table 5). However, Ni, Zn, Sr, and Co are depleted (Table 5).

Early Cambrian black shales exhibit strongly enriched Se, Ga, and As, significantly enriched Ba, Bi, and Rb,

weakly enriched Mo, Cs, Cd, V, U, Be, In, and Tl, normal Sc, Th, Cr, Li, Cu, Ni, and Pb and depleted Co, Zn, and Sr (Fig. 2, Table 5).

4.3 Variation between the Se concentrations of Ediacaran and early Cambrian black shales

The Ediacaran and early Cambrian black shales in the Yangtze block generally exhibit high Se concentrations. For instance, the Se content in the black shales of the Ediacaran Lantian Formation, southern Anhui Province, is as high as 94.77 ppm and averaging 5.95 ppm (Li Shuangying, 1994). The Se content in the black shales of the Ediacaran Doushantuo member IV is as high as 25.08 ppm with arithmetic mean value of 12.49 ppm in the Yangtze Gorges area, Hubei Province (Tian et al., 2017a; Tian Xinglei and Luo Kunli, 2017b). The black shales of the early Cambrian Niutitang Formation exhibit the high Se contents of 223.85 and 164.44 ppm in Taoyuan Country, Hunan Province (Ni et al., 2015) and Zunyi region, Guizhou Province (Fan et al., 2011), respectively.

The Ediacaran and early Cambrian black shales in this study area in Cathaysia also are enriched in Se. Se is the most enriched trace element in the Ediacaran and early Cambrian black shales, the concentrations of Se vary from 0.25 to 30.09 ppm and 0.54 to 5.01 ppm (Table 5), with average values of 4.84 ± 6.28 ppm ($n = 34$) and 1.72 ± 1.45 ppm ($n = 13$), and average EF values of 96.87 and 34.32, respectively. The maximum reported value of Se occurred in the Ediacaran black shale, and the average content of Se in the Ediacaran black shales are 2.8 times of early Cambrian black shales.

Variance analysis shows that there are significant differences between the Se contents in the Ediacaran and early Cambrian black shales ($P = 0.03$). In the following sections, the origin of the high Se contents in the Ediacaran and early Cambrian black shales in this study area are discussed.

4.4 Origin of the enriched Selenium

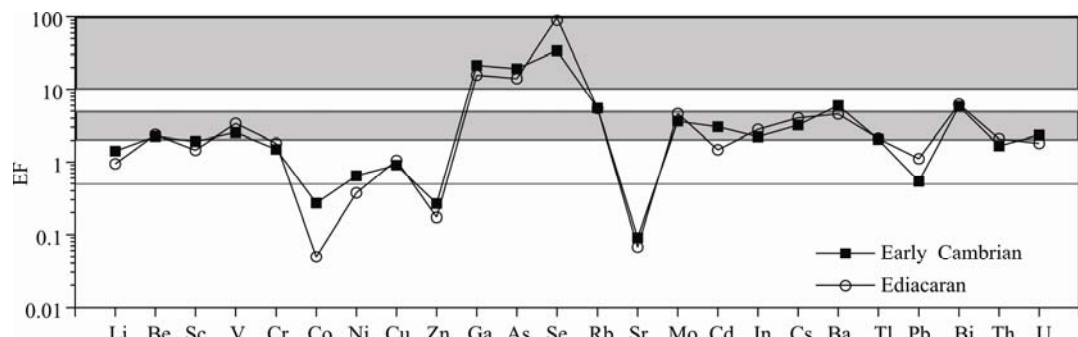


Fig. 2. Trace element enrichment factors (EF) relative to Upper Continental Crust (McLennan, 2001) of the Ediacaran and early Cambrian black shales in the Guangning area, western Guangdong Province, South China.

4.4.1 Effect of terrigenous input

Detrital and authigenic components contribute to the trace element concentrations in bulk black shales (Tribovillard et al., 2006). An effective method to check whether the content of a given element is dominantly controlled by the detrital flux is to plot this trace element versus aluminum (Al) or thorium (Th), which can be considered as an indicator of the aluminosilicate fraction of the sediments, which is not mobile during diagenesis (Tribovillard et al., 2006; Schröder and Grotzinger, 2007; Tian Xinglei and Luo Kunli, 2017a). A good correlation of the observed trace elements with Al or Th would suggest that the trace elements are of detrital provenance (Tribovillard et al., 2006). Correlation analysis showed that no significant positive correlations between Se with Al or Th in both Ediacaran ($r_{\text{Se-Al}}=0.23$; $r_{\text{Se-Th}}=0.04$) and early Cambrian ($r_{\text{Se-Al}}=0.36$; $r_{\text{Se-Th}}=0.24$) black shales, which suggest that Se was not of detrital provenance.

4.4.2 Effect of hydrothermal fluids

Eu is the only rare earth element that can be reduced from Eu^{3+} to Eu^{2+} (Brookins, 1989). Positive Eu anomalies in shallow seawater may not reflect the redox state of waters, but are always associated with high temperature ($>250^\circ\text{C}$) (Sverjensky, 1984) and reducing hydrothermal fluid (Michard and Albarède, 1986; Olivarez and Owen, 1991; Bau and Dulski, 1996; Kamber and Webb, 2001). Nearly all the studied black shales show slight positive Eu anomalies (<1.5) (Table 5). Furthermore, slight positive Eu anomalies were commonly observed in the Ediacaran and early Cambrian strata throughout the Yangtze platform (Guo et al., 2007; Tian Xinglei and Luo Kunli, 2017a). This observation indicates that the weak positive Eu anomaly is a common phenomenon in the Ediacaran and early Cambrian period around South China. Weak positive Eu anomalies also suggest that deposits were not directly transformed by hydrothermal flux. A mixture of hydrothermal flux and seawater possibly led to the weak positive Eu anomalies, which are preserved by authigenic

Table 1 Major elements oxides compositions (wt%), LOI (wt%), S (ppm), U/AI (ppm%), V/AI (ppm%), Mo/AI (ppm%), and Co/Zn of the investigated black shales in the Guangning area, western Guangdong Province, South China

Sample	Section	Unit	Depth(m)	SiO ₂	LOI	Al ₂ O ₃	CaO	Fe ₂ O ₃	K ₂ O	Na ₂ O	MgO	P ₂ O ₅	TiO ₂	S	U/AI	V/AI	Mo/AI	Co/Zn	
GS-10	GY	LPBG	25.82	72.49	4.39	15.34	0.07	2.44	3.49	0.12	0.94	0.012	0.02	0.70	751.8	0.36	12.18	0.06	0.13
GS-9	GY	LPBG	25.06	66.02	4.83	19.16	0.11	2.87	5.14	0.13	0.92	0.011	0.03	0.79	301.3	0.47	14.25	0.04	0.87
GS-8	GY	LPBG	18.61	65.86	4.08	18.36	0.05	3.74	5.62	0.11	1.34	0.005	0.05	0.80	244.6	0.91	46.28	0.76	0.05
GS-7	GY	LPBG	16.71	65.02	3.82	18.39	0.08	4.64	5.70	0.12	1.30	0.008	0.03	0.90	302.2	0.94	27.05	0.73	0.12
GS-6	GY	LPBG	12.91	80.27	2.63	11.0	0.11	1.27	3.26	0.10	0.73	0.010	0.04	0.59	287.6	0.92	14.84	2.96	0.26
GS-5	GY	LPBG	6.84	68.91	4.19	18.97	0.04	4.44	4.72	0.12	0.80	0.005	0.03	0.78	169.2	0.47	13.79	0.06	0.18
GS-4	GY	LPBG	5.71	71.15	3.56	16.57	0.05	1.20	5.34	0.10	1.28	0.005	0.03	0.72	165.6	1.26	58.22	0.61	
GS-3	GY	LPBG	4.08	70.40	3.75	17.36	0.21	1.72	4.75	0.14	0.87	0.007	0.03	0.78	507.1	0.57	28.10	0.08	0.23
GS-2	GY	LPBG	3.26	69.58	4.17	17.79	0.16	2.09	4.51	0.12	0.84	0.002	0.01	0.73	392.1	0.44	14.71	0.03	0.07
GS-1	GY	LPBG	0	70.23	3.80	17.36	0.05	2.15	4.65	0.09	0.94	0.004	0.02	0.71	179.9	0.43	17.80	0.05	0.14
MEL-4		LPBG	60.60	8.30	18.50	0.10	4.12	5.29	0.15	1.97	0.022	0.06	0.89	10780	0.96	61.47	1.51	0.29	
MEL-5		LPBG	74.25	4.37	13.71	0.15	1.58	3.62	0.12	1.26	0.016	0.08	0.85	927.7	1.37	46.58	1.11	0.26	
MEL-6		LPBG	63.23	7.56	17.74	0.09	3.57	4.80	0.11	2.11	0.022	0.01	0.75	2220	0.59	33.70	0.82	0.22	
ZB-34	LW	UPLG	37.55	58.59	8.36	22.43	0.11	1.56	6.54	0.22	1.21	0.003	0.02	0.96	229.4	0.43	26.82	0.46	0.03
ZB-33	LW	UPLG	35.55	57.50	7.10	23.70	0.09	3.26	6.16	0.23	1.07	0.005	0.01	0.88	401.1	0.34	19.14	0.22	0.04
ZB-32	LW	UPLG	34.27	63.09	7.18	17.83	0.08	4.56	5.28	0.17	0.97	0.004	0.01	0.81	265.6	0.61	95.58	2.16	0.05
ZB-31	LW	UPLG	32.57	58.73	9.34	19.51	0.07	4.29	5.85	0.17	1.05	0.004	0.02	0.96	210.6	0.95	173.79	6.62	0.09
ZB-30	LW	UPLG	30.01	58.82	6.10	21.09	0.07	6.33	5.43	0.18	0.95	0.003	0.04	0.98	361.2	0.69	24.46	0.15	0.03
ZB-29	LW	UPLG	29.16	65.99	5.17	19.80	0.09	2.05	4.91	0.18	0.81	0.002	0.02	0.97	273.7	0.50	19.17	0.08	0.09
ZB-28	LW	UPLG	28.06	64.66	4.72	21.47	0.08	1.80	5.34	0.20	0.81	0.001	0.01	0.90	217.1	0.35	15.02	0.03	0.06
ZB-27	LW	UPLG	27.46	68.98	4.18	18.80	0.06	1.53	4.72	0.17	0.76	0.002	0.01	0.80	166.3	0.49	15.90	0.05	0.09
ZB-26	LW	UPLG	25.50	66.94	4.61	19.50	0.09	2.31	4.82	0.19	0.76	0.002	0.03	0.74	301.7	0.29	13.53	0.01	0.19
ZB-25	LW	UPLG	24.48	65.77	4.49	20.39	0.11	2.26	5.21	0.21	0.85	0.002	0.03	0.74	379.4	0.27	13.90	0.02	0.40
ZB-24	LW	UPLG	22.35	80.36	3.80	9.64	0.04	2.84	2.24	0.09	0.44	0.003	0.04	0.51	238.6	0.57	13.44	0.39	
ZB-23	LW	UPLG	21.74	58.57	6.61	24.78	0.08	1.15	6.48	0.19	1.17	0.005	0.04	0.91	244.4	0.46	48.45	0.33	0.08
ZB-22	LW	UPLG	20.84	67.61	4.61	19.46	0.10	1.28	5.09	0.17	0.87	0.003	0.01	0.79	250	0.41	14.61	0.06	0.31
ZB-21	LW	UPLG	19.33	58.28	7.62	23.62	0.11	1.53	6.64	0.21	1.24	0.003	0.01	0.74	291.5	0.45	80.29	1.51	1.48
ZB-20	LW	UPLG	18.72	61.12	5.14	19.63	0.06	6.61	5.50	0.18	0.95	0.004	0.02	0.79	409.7	0.49	15.54	0.34	
ZB-19	LW	UPLG	17.52	71.83	4.32	16.30	0.07	1.88	4.02	0.16	0.67	0.003	0.01	0.74	314.2	0.51	14.43	0.02	0.67
ZB-18	LW	UPLG	16.61	55.42	6.60	23.71	0.08	5.98	6.05	0.19	1.00	0.003	0.03	0.94	466	0.44	15.21	0.08	0.07
ZB-17	LW	UPLG	16.01	60.94	6.09	20.30	0.09	4.41	5.89	0.18	1.09	0.004	0.03	0.98	236.5	0.45	28.70	0.52	0.04
ZB-16	LW	UPLG	14.62	69.19	4.88	16.03	0.04	4.38	3.95	0.13	0.68	0.004	0.03	0.68	324.2	0.42	17.96	0.17	0.10
ZB-15	LW	UPLG	13.89	60.34	5.59	21.55	0.11	4.37	5.97	0.20	0.98	0.004	0.06	0.83	411.1	0.41	15.19	0.04	0.13
ZB-14	LW	UPLG	12.68	68.03	6.98	17.58	0.09	1.0	4.61	0.14	0.81	0.003	0.01	0.76	204.8	0.42	44.94	0.41	0.07
ZB-13	LW	UPLG	12.08	57.50	7.37	16.78	0.08	11.86	4.58	0.15	0.79	0.005	0.10	0.79	402.8	1.03	66.69	1.96	
ZB-12	LW	UPLG	10.99	62.72	8.75	18.86	0.09	2.33	5.26	0.16	0.93	0.004	0.01	0.88	334.6	0.57	51.87	1.40	3.27
ZB-11	LW	UPLG	9.79	67.77	6.85	17.17	0.04	1.0	5.20	0.15	0.93	0.003	0.01	0.88	187.4	0.64	21.82	1.21	
ZB-10	LW	UPLG	8.46	61.76	5.89	21.76	0.07	3.04	5.64	0.16	0.96	0.004	0.01	0.71	280.7	0.43	15.49	0.22	0.06
ZB-9	LW	UPLG	7.85	65.62	5.86	17.41	0.73	0.73	5.72	2.02	1.03	0.004	0.00	0.87	373	0.46	29.42	0.32	1.25
ZB-8	LW	UPLG	6.34	63.44	6.94	18.66	0.08	4.35	4.80	0.14	0.86	0.004	0.01	0.72	371.2	0.51	26.68	0.87	0.09
ZB-7	LW	UPLG	5.80	61.96	6.22	20.80	0.14	3.01	5.83	0.17	1.02	0.004	0.01	0.85	321.2	0.51	31.55	0.14	
ZB-6	LW	UPLG	5.13	62.61	6.99	21.38	0.08	1.17	5.73	0.16	1.03	0.004	0.01	0.84	304.4	0.47	31.01	0.21	0.04
ZB-5	LW	UPLG	4.05	63.65	6.45	20.73	0.10	5.94	0.18	1.02	0.004	0.01	0.83	268.7	0.50	73.90	0.21	0.05	
ZB-4	LW	UPLG	2.42	64.14	5.42	20.57	0.10	2.07	5.65	0.18	1.00	0.004	0.01	0.85	410.2	0.55	46.01	0.48	0.08
ZB-3	LW	UPLG	1.81	62.39	5.15	18.43	0.08	6.88	5.09	0.20	0.88	0.006	0.05	0.85	422.2	0.54	28.68	1.05	0.02
ZB-2	LW	UPLG	0.60	69.03	3.91	16.48	0.12	4.31	4.58	0.19	0.75	0.006	0.03	0.61	434.9	0.37	15.66	0.95	0.07
ZB-1	LW	UPLG	0	66.10	4.14	19.46	0.15	2.93	5.18	0.23	0.84	0.008	0.02	0.96	437.6	0.32	16.81	0.70	0.04

Note: LW, Linwu; GY, Guanyang; UPLG, Upper part of Lechangxia Group; LPBG, Lower part of Bacun Group. The PAAS data from (Taylor and McLennan, 1985; McLennan, 2001).

Table 2 Trace elements concentrations (ppm) of the investigated black shales in the Guangming area, western Guangdong Province, South China

Sample	Li	Be	Sc	V	Cr	Co	Ni	Cu	Zn	Ga	As	Se	Rb	Sr	Mo	Cd	In	Cs	Ba	Tl	Pb	Bi	Th	U	
GS-10	74.15	5.35	20.80	98.88	102.50	3.25	37.30	17.85	25.26	248.41	34.03	0.54	468.21	26.60	0.47	0.89	0.09	9.66	1460.0	0.93	7.22	0.27	13.33	2.96	
GS-9	26.42	7.74	28.37	144.50	124.0	20.77	38.76	59.93	23.90	344.58	17.77	0.76	684.09	42.09	0.38	0.87	0.14	13.89	1.42	1.84	1.86	18.97	4.79		
GS-8	30.80	8.14	28.11	449.80	194.0	0.68	10.68	35.95	15.05	447.73	159.95	2.16	762.17	42.91	7.37	0.12	0.13	15.63	3603.0	1.76	3.73	0.33	21.39	8.85	
GS-7	34.87	8.66	28.42	263.40	144.90	1.03	11.49	34.18	8.90	438.79	36.53	4.56	776.79	29.96	7.15	0.17	0.10	15.44	3627.0	1.88	ND	0.34	21.39	9.14	
GS-6	18.82	5.03	18.19	86.44	80.97	ND	3.92	2.87	208.34	21.63	0.85	484.98	44.74	29.56	17.26	0.11	0.08	9.61	1674.0	0.99	9.13	0.50	13.72	5.33	
GS-5	18.42	6.80	26.77	138.50	95.48	1.66	60.69	3.49	9.35	215.19	34.37	0.90	634.56	44.74	0.56	0.23	0.13	13.04	2093.0	1.36	0.42	0.54	17.86	4.68	
GS-4	25.13	6.47	26.14	510.70	109.20	0.42	ND	ND	ND	398.73	2.33	1.23	726.56	34.41	5.36	0.12	0.07	15.97	3273.0	1.78	6.68	0.42	17.93	11.05	
GS-3	17.0	6.28	26.77	238.50	132.60	6.57	28.08	18.68	28.43	461.87	34.08	0.80	670.57	27.93	0.78	0.17	0.12	13.02	4276.0	1.66	ND	0.56	19.30	5.20	
GS-2	42.55	5.97	27.24	138.50	106.30	1.20	5.49	21.38	17.26	497.53	3.94	0.79	462.68	33.45	0.32	0.19	0.13	13.11	4598.0	1.44	ND	0.30	19.45	4.13	
GS-1	19.21	6.85	25.45	163.60	102.50	1.61	40.48	28.57	11.90	496.64	13.40	1.99	652.81	23.14	0.43	0.11	0.12	15.36	4676.0	1.53	ND	1.11	19.78	3.92	
MEL-4	23.67	7.41	32.96	602.0	201.60	9.61	46.24	10.81	32.83	507.03	4.28	5.01	683.29	18.42	14.76	0.22	0.11	22.21	4642.0	2.02	9.34	0.91	16.83	9.39	
MEL-5	14.34	8.13	24.45	338.10	95.86	6.94	13.94	25.74	26.59	257.28	1.96	1.01	394.01	40.46	8.09	0.50	0.10	15.64	2880.0	1.33	40.82	1.42	21.62	9.96	
MEL-6	22.99	5.22	25.79	316.50	131.20	5.06	19.36	10.89	22.55	255.75	14.15	1.71	646.17	15.91	7.73	0.15	0.12	13.02	4276.0	1.76	3.60	1.32	14.05	5.50	
ZB-33	26.18	9.0	23.29	318.50	108.20	0.77	4.61	0.93	24.89	504.41	4.04	0.87	688.86	22.19	5.49	0.13	0.13	13.11	4236.0	1.85	12.57	1.40	26.45	5.09	
ZB-34	23.76	9.44	24.22	240.20	140.10	1.05	16.48	43.79	26.52	500.73	7.25	4.71	843.92	21.56	2.82	0.13	0.19	23.71	4157.0	1.84	18.97	1.12	27.42	4.27	
ZB-32	19.86	7.32	17.31	902.20	155.0	0.61	11.46	25.0	12.59	266.03	2.83	3.82	737.16	18.90	20.42	0.17	0.13	21.20	3067.0	1.74	2.38	0.56	21.91	5.72	
ZB-31	24.17	8.11	19.67	179.50	217.70	0.73	18.72	31.19	8.07	411.33	9.22	8.59	833.54	19.79	68.42	0.29	0.23	24.93	3361.0	1.87	51.79	1.84	25.56	9.80	
ZB-30	18.95	8.09	19.11	273.10	300.10	1.10	29.61	12.86	32.27	404.88	10.09	19.10	737.67	24.98	1.68	0.19	0.16	21.14	3033.0	1.59	3408.0	1.76	31.35	7.70	
ZB-29	15.39	9.47	21.15	200.90	138.60	1.16	12.80	10.26	13.35	402.03	25.86	2.72	694.30	27.92	0.84	0.20	0.16	17.89	2584.0	1.40	5.40	0.39	24.04	5.29	
ZB-28	17.04	8.65	20.59	170.70	133.90	0.87	14.09	ND	15.34	393.81	18.49	3.54	727.85	32.47	0.29	0.18	0.18	18.18	3027.0	1.48	4.78	0.20	24.04	3.95	
ZB-27	14.05	7.07	17.96	158.30	119.50	1.27	14.89	ND	14.53	244.42	10.10	1.16	606.10	25.72	0.46	0.21	0.14	16.78	2580.0	1.30	ND	0.19	25.77	4.83	
ZB-26	14.80	8.29	19.27	139.70	115.50	1.15	17.30	7.71	5.94	384.57	5.61	1.97	647.55	27.77	0.11	0.13	0.15	15.71	2721.0	1.37	ND	0.39	24.66	2.98	
ZB-25	16.63	9.04	20.10	150.0	125.10	0.94	17.30	3.74	2.36	389.47	5.27	661.99	28.06	0.23	0.13	0.14	16.67	2839.0	1.42	ND	0.27	21.66	2.93		
ZB-24	7.50	2.69	11.77	68.57	93.0	0.66	17.71	16.96	ND	125.04	7.74	5.32	161.21	17.84	0.98	0.09	0.09	8.12	1087.0	0.64	25.85	0.47	11.32	2.91	
ZB-22	22.56	6.87	25.44	635.60	170.0	0.89	21.74	15.83	10.94	392.18	7.36	9.29	818.84	32.03	4.38	0.14	0.13	22.73	3150.0	1.81	60.03	1.52	20.10	6.0	
ZB-21	19.15	6.17	19.43	150.50	121.60	1.08	22.82	4.92	3.52	327.35	21.45	1.39	629.93	20.73	0.61	0.08	0.13	15.93	2471.0	1.41	2.87	0.69	27.87	4.24	
ZB-20	21.88	7.74	27.66	1004.0	159.0	0.68	7.72	21.69	0.46	163.53	5.66	1.09	381.49	22.99	18.93	0.12	0.14	23.12	3018.0	1.71	25.17	0.82	21.06	5.61	
ZB-19	17.73	7.10	18.82	161.50	158.20	0.48	19.87	60.85	6.68	224.86	3.74	2.50	661.99	20.48	3.57	0.10	0.14	18.0	2420.0	1.46	2420.0	0.88	21.95	5.09	
ZB-18	13.54	5.32	16.37	124.50	104.60	1.37	180.55	64.13	1.57	248.92	20.64	2.21	0.09	0.15	12.57	1750.0	1.07	ND	0.32	16.60	4.39				
ZB-17	23.28	7.54	23.30	308.40	160.70	0.65	17.36	46.76	12.05	358.69	63.23	1.59	736.92	30.52	1.06	0.04	0.15	18.64	2896.0	1.58	1.20	0.28	27.44	5.49	
ZB-16	13.46	4.80	15.70	152.40	116.0	1.17	19.62	11.99	11.65	94.59	57.99	2.91	224.86	18.22	1.46	0.06	0.11	12.08	1776.0	1.05	11.83	0.78	23.77	4.86	
ZB-15	20.84	8.26	22.34	173.30	150.90	0.54	13.98	7.57	4.21	243.12	19.89	1.73	696.19	30.09	0.41	0.16	0.16	19.12	2839.0	1.62	17.22	0.34	27.35	4.67	
ZB-14	18.85	5.86	16.62	418.30	132.30	0.54	11.88	6.40	7.27	168.95	3.77	2.62	584.22	16.88	3.86	0.13	0.11	17.46	1880.0	1.52	4.83	0.54	17.28	3.89	
ZB-13	16.59	5.60	17.01	592.70	239.20	0.52	14.12	115.27	112.84	18.35	661.28	14.49	17.39	19.17	16.94	8.55	0.10	0.13	16.38	1803.0	1.44	19.18	1.06	18.57	5.08
ZB-12	19.08	6.22	19.39	517.90	154.70	0.49	8.21	14.23	0.15	187.31	40.91	3.40	330.30	20.62	13.94	0.14	0.16	17.94	1986.0	1.71	3.45	0.78	23.36	5.67	
ZB-11	19.75	6.88	19.53	198.30	101.0	0.39	1.25	ND	ND	195.12	11.75	0.54	523.99	19.06	11.04	0.12	0.12	20.13	1941.0	1.84	2.55	0.86	22.85	5.81	
ZB-10	19.48	7.16	19.18	178.50	114.60	0.75	22.58	20.96	11.89	204.27	7.61	1.07	702.79	18.28	2.56	0.10	0.14	20.06	2184.0	1.72	0.58	0.63	22.58	4.94	
ZB-9	22.32	4.64	19.23	271.20	99.46	1.30	25.97	ND	1.30	284.79	ND	0.25	486.42	61.12	2.91	0.16	0.13	17.50	4576.0	1.47	ND	0.94	18.79	4.21	
ZB-8	18.38	6.16	17.77	263.60	150.10	1.32	29.45	62.56	14.12	115.27	4.0	8.04	296.71	16.94	8.55	0.10	0.13	16.38	1803.0	1.44	19.18	1.06	18.57	5.08	
ZB-7	19.06	7.68	20.88	347.40	171.50	0.63	10.29	7.88	6.70	300.50	18.40	3.52	711.99	19.62	1.54	0.15	0.15	19.76	2198.0	1.65	ND	0.46	22.82	5.58	
ZB-6	20.86	8.75	19.62	351.0	128.20	0.62	8.05	2.54	13.85	291.26	3.63	0.77	716.22	19.25	2.42	0.15	0.13	21.05	2114.0	1.70	ND	0.30	24.42	5.33	
ZB-5	19.15	5.77	20.51	811.0	184.50	0.51	3.08	6.07	11.17	112.48	1.0	0.78	313.53	19.19	2.27	0.14	0.12	17.82	2273.0	1.65	ND	0.53	23.06	5.53	
ZB-4	20.86	6.36	19.91	501.10	161.50	0.95	10.82	71.24	26.94	46.63	4.63	8.04	6.62	783.22	18.58	5.26	0.22	0.13	20.91						

Table 3 REE concentrations (ppm) and Eu/Eu* values of the investigated black shales in the Guangning area, western Guangdong Province, South China

Sample	La	Ce	Pr	Nd	Sm	Eu	Gd	Tb	Dy	Ho	Y	Er	Tm	Yb	Lu	Eu/Eu*
GS-10	36.65	70.18	8.13	32.48	6.84	1.43	5.83	0.64	3.10	0.55	13.91	1.56	0.22	1.54	0.24	1.07
GS-9	53.51	99.06	11.15	44.90	8.83	2.15	7.38	0.78	3.84	0.68	18.05	2.07	0.32	2.24	0.36	1.25
GS-8	60.66	105.14	13.06	52.40	10.55	2.60	8.54	0.92	4.77	0.89	25.0	2.74	0.40	2.88	0.47	1.29
GS-7	58.15	111.55	12.65	52.34	10.34	2.63	7.98	0.81	3.77	0.72	20.01	2.28	0.35	2.48	0.43	1.36
GS-6	42.85	75.26	9.35	38.37	7.86	1.75	6.44	0.71	3.58	0.67	18.37	2.02	0.29	2.02	0.30	1.16
GS-5	57.18	104.11	12.33	48.42	8.76	1.88	7.32	0.79	3.78	0.71	18.14	2.06	0.29	2.06	0.33	1.11
GS-4	41.75	76.24	9.20	36.70	7.82	2.01	5.90	0.65	3.37	0.64	17.56	2.06	0.31	2.54	0.40	1.39
GS-3	78.39	145.05	20.42	89.49	17.19	3.45	12.88	1.37	6.81	1.23	33.06	3.61	0.53	3.57	0.55	1.09
GS-2	47.78	87.96	10.39	41.22	9.20	2.30	7.04	0.71	3.45	0.63	16.70	1.91	0.29	2.35	0.36	1.34
GS-1	54.10	101.57	12.21	49.70	10.28	2.46	7.43	0.79	3.70	0.68	18.42	2.14	0.32	2.40	0.39	1.32
MEL-4	70.02	201.34	16.14	43.93	10.19	2.62	7.27	0.72	3.65	0.68	19.12	2.40	0.36	2.84	0.50	1.43
MEL-5	60.07	104.86	13.55	54.64	12.16	2.57	9.06	0.98	4.78	0.85	31.03	2.58	0.36	2.69	0.46	1.15
MEL-6	40.66	71.70	9.24	36.53	7.96	1.95	6.02	0.63	3.07	0.55	22.84	1.84	0.29	2.34	0.40	1.32
ZB-34	73.48	115.60	17.35	68.41	14.47	3.58	11.57	1.29	6.36	1.14	30.16	3.47	0.50	3.54	0.57	1.30
ZB-33	73.71	110.69	16.21	63.07	13.53	3.12	9.22	0.82	2.98	0.43	10.43	1.33	0.20	1.63	0.33	1.31
ZB-32	58.31	104.71	13.74	55.20	11.27	2.96	8.23	0.79	3.39	0.56	15.88	1.73	0.26	2.09	0.37	1.44
ZB-31	68.95	111.21	18.13	72.76	15.81	3.98	12.13	1.34	6.95	1.36	42.51	4.39	0.64	4.68	0.79	1.35
ZB-30	156.82	216.75	40.58	166.52	32.48	5.58	23.41	2.11	7.39	0.92	28.93	2.47	0.32	2.42	0.40	0.95
ZB-29	130.23	234.37	33.23	135.80	21.36	4.98	15.20	1.41	6.04	0.92	22.29	2.62	0.36	2.66	0.45	1.30
ZB-28	71.21	113.74	15.86	61.57	11.21	2.87	9.32	1.0	4.86	0.83	21.50	2.44	0.34	2.59	0.41	1.32
ZB-27	62.53	110.01	14.32	55.80	10.24	2.56	8.31	0.84	3.77	0.61	14.84	1.80	0.27	1.98	0.31	1.31
ZB-26	78.22	103.28	16.32	63.98	12.56	3.09	11.27	1.12	4.57	0.68	16.79	1.93	0.27	2.06	0.34	1.22
ZB-25	71.15	100.29	16.23	64.26	11.81	2.76	9.07	0.95	4.12	0.65	16.14	1.96	0.28	2.07	0.34	1.25
ZB-24	110.83	75.49	24.02	89.09	15.82	2.60	9.63	0.86	3.0	0.38	7.61	1.11	0.13	1.0	0.16	0.98
ZB-23	141.72	98.22	33.21	124.55	22.29	4.44	14.29	1.36	4.71	0.62	12.77	1.81	0.23	1.85	0.33	1.16
ZB-22	75.93	111.72	15.84	59.30	10.43	2.31	7.91	0.73	2.89	0.43	10.42	1.32	0.21	1.58	0.28	1.20
ZB-21	85.42	123.03	17.32	64.59	12.06	2.66	8.80	0.76	2.77	0.38	9.08	1.12	0.18	1.62	0.31	1.21
ZB-20	55.70	84.06	11.57	44.23	8.50	1.94	6.33	0.59	2.32	0.36	8.42	1.10	0.18	1.44	0.26	1.24
ZB-19	44.29	78.11	9.47	37.17	7.29	1.66	5.90	0.60	2.55	0.41	9.84	1.20	0.19	1.37	0.24	1.19
ZB-18	67.85	128.28	15.42	63.92	15.22	3.27	12.0	1.13	4.38	0.63	14.03	1.68	0.23	1.83	0.31	1.14
ZB-17	75.66	144.45	16.93	64.59	11.50	2.80	8.85	0.79	3.06	0.43	9.81	1.34	0.19	1.61	0.29	1.31
ZB-16	56.68	106.38	12.53	48.45	9.53	1.99	7.50	0.72	2.70	0.36	12.69	1.01	0.15	1.12	0.19	1.11
ZB-15	99.05	167.31	23.80	99.64	22.77	3.83	16.77	1.51	5.70	0.83	20.02	2.23	0.31	2.29	0.39	0.92
ZB-14	56.08	95.32	12.94	51.99	10.47	2.17	8.11	0.82	3.60	0.60	15.35	1.81	0.27	2.02	0.35	1.11
ZB-13	43.32	96.35	10.81	44.37	9.50	1.88	7.35	0.71	3.15	0.52	13.36	1.69	0.24	6.18	0.31	1.06
ZB-12	65.27	122.56	15.87	63.95	13.21	2.54	9.71	0.94	3.86	0.58	15.53	1.81	0.26	2.07	0.34	1.05
ZB-11	67.46	128.19	16.30	65.01	12.97	2.76	9.58	0.91	3.70	0.56	15.12	1.75	0.26	1.92	0.33	1.16
ZB-10	59.87	112.96	13.73	54.06	10.01	2.18	7.42	0.69	2.59	0.38	9.04	1.14	0.17	1.37	0.26	1.19
ZB-9	57.68	109.96	12.62	50.57	10.50	2.66	9.04	0.74	2.87	0.43	11.43	2.91	0.20	1.59	0.30	1.29
ZB-8	47.21	87.93	10.63	41.97	8.64	1.87	6.75	0.67	2.86	0.47	11.80	1.43	0.21	1.65	0.29	1.15
ZB-7	70.44	117.84	15.68	62.06	11.85	2.64	9.83	0.90	3.53	0.56	14.57	1.65	0.24	1.88	0.34	1.15
ZB-6	71.75	129.94	16.35	65.12	12.25	2.64	9.82	0.94	3.54	0.52	19.43	1.52	0.22	1.70	0.30	1.13
ZB-5	73.76	123.81	16.69	68.21	13.87	2.75	10.86	0.99	9.19	0.52	13.28	1.51	0.22	1.78	0.30	1.05
ZB-4	60.12	102.85	14.14	58.26	11.25	2.42	9.64	0.91	3.90	0.66	18.13	2.02	0.30	2.27	0.39	1.09
ZB-3	36.45	75.44	8.17	32.24	6.39	1.61	5.20	0.51	2.28	0.39	10.27	1.21	0.18	1.48	0.25	1.32
ZB-2	45.45	88.0	10.06	40.17	7.90	1.83	6.05	0.61	2.32	0.35	8.75	1.03	0.15	1.19	0.21	1.25
ZB-1	48.21	90.68	10.43	39.67	7.23	1.88	6.14	0.59	2.60	0.42	10.37	1.27	0.18	1.48	0.27	1.33

sediments (Derry and Jacobsen, 1990). However, the stability field of Eu²⁺ could also be reached under euxinic environment as in the modern Black sea (Sverjensky, 1984). Thus, the depositional environment of the Ediacaran and early Cambrian black shales must be constrained.

The trace elements U, V, and Mo are good indicators of redox conditions. The use of enrichment ratios (e.g., U/Al, V/Al and Mo/Al ratios) relative to certain shale standards (PAAS or Black Sea euxinic sediment) has been extended

from modern sediments to ancient shales (Algeo and Maynard, 2004; Lyons et al., 2009; Pi et al., 2013). In the following sections, we will use these proxies to explore the depositional environment.

Before discerning redox conditions, the following considerations should be made first. Only the concentrations of authigenic components are response to redox changes in the water column (Tribouillard et al., 2006). An effective method to check the authigenic enrichment of a given element is to normalize it to Al,

Table 4 Statistics values for major element oxides, LOI, and S

	SiO ₂	LOI	Al ₂ O ₃	CaO	MgO	Fe ₂ O ₃	K ₂ O	MnO	Na ₂ O	P ₂ O ₅	TiO ₂	S
C ₁	Maximum	80.27	8.30	19.16	0.21	2.11	4.64	5.70	0.022	0.15	0.08	0.90
	Minimum	60.60	2.63	11.0	0.04	0.73	1.20	3.26	0.002	0.09	0.01	0.59
	Average	69.08	4.57	16.94	0.10	1.18	2.53	4.68	0.010	0.12	0.03	1325.32
	SD	5.11	1.58	2.34	0.05	0.44	1.16	0.79	0.007	0.02	0.02	2894.72
	Median	69.58	4.17	17.74	0.09	0.94	2.15	4.75	0.010	0.12	0.03	302.2
E	Maximum	80.36	9.34	24.78	0.73	1.24	11.86	6.64	0.008	2.02	0.10	0.98
	Minimum	55.42	3.80	9.64	0.04	0.44	0.73	2.24	0.001	0.09	0.01	0.51
	Average	63.81	5.98	19.58	0.11	0.92	3.24	5.29	0.004	0.23	0.02	316.06
	SD	4.99	1.42	2.85	0.11	0.16	2.32	0.85	0.001	0.32	0.02	82.98
	Median	63.27	5.99	19.57	0.09	0.94	2.59	5.31	0.004	0.18	0.02	309.3
PAAS	Average	62.80		18.90	1.29	2.19	7.18	3.68	0.110	1.19	0.16	0.99

Note: C₁-early Cambrian; E-Ediacaran; SD-standard deviation. The unit of maximum, minimum, average, SD, and median for major element oxides and LOI is %, and for S is mg/kg. The data for PAAS are according to Taylor and McLennan (1985) and McLennan (2001).

which can be an indicator of detrital origin and is usually immobile during diagenesis (Algeo and Maynard, 2004; Tribouillard et al., 2006; Schröder and Grotzinger, 2007). If Al originates from relatively Al-rich or poor sources, the enrichment can be overestimated or underestimated (Kryc et al., 2003). A standard method of estimating whether Al comes from a common siliciclastic flux is to plot Al versus scandium (Sc), thorium (Th) or zirconium (Zr), which are also usually derived from a detrital source. A strong correlation may suggest that Al comes from a common siliciclastic source. Following this logic, we calculated the correlations of Al versus Sc and Th. Results show that Al exhibits significant positive correlations with Th or Sc in the Ediacaran ($r_{\text{Al-Th}}=0.64$, $r_{\text{Al-Sc}}=0.88$; $P<0.01$) and early Cambrian ($r_{\text{Al-Sc}}=0.83$; $P<0.01$) black shales, indicating that Al originated from a normal siliciclastic flux. Thus, using the Al-normalized procedure to look for trace element enrichments beyond the detrital flux is justified.

Uranium (U) exists as soluble U⁶⁺ under oxidizing condition. However, under highly reducing conditions, U⁶⁺ is reduced to the insoluble U⁴⁺ and precipitates into the sediments as crystalline uraninite (UO₂) or its metastable precursors under certain reducing conditions (Calvert and Pedersen, 1993). The U/Al ratios (ppm %) of the Ediacaran and early Cambrian black shales range from 0.27 to 1.03 and 0.36 to 1.37 with an average value of 0.49 ± 0.16 ($n = 34$) and 0.74 ± 0.34 ($n = 3$), respectively. These values are a slightly higher than that of the PAAS (0.31) (Taylor and McLennan, 1985) and lower than that of Black Sea euxinic sediment (3.3) (Calvert and Pedersen, 1993) (Fig. 3).

Vanadium is a redox sensitive element which is preferentially enriched in sediments underlying anoxic or near anoxic waters (Calvert and Pedersen, 1993). In the present study, the V/Al ratios ((ppm)/%) of the Ediacaran black shales range from 13.44 to 173.79 and the average value is 34.75 ± 32.45 ($n=34$). These values are within the V/Al ratios of PAAS (15.0) (Taylor and McLennan, 1985) and Black Sea euxinic sediment (28.8) (Calvert and Pedersen, 1993), whereas a little part hold the higher V/Al

ratios than 28.8 (Fig. 3). The similar variation of V/Al ratios could be detected in the early Cambrian black shales (Fig. 3).

Molybdenum is conservative under the oxic marine environment (Algeo and Lyons, 2006). Its removal from the water column to sediments requires a reduction reaction through which H₂S/HS⁻ transforms stable molybdate to particle-reactive thiomolybdates (Helz et al., 1996). The Mo/Al ratios (ppm %) of the Ediacaran and early Cambrian black shales range from 0.27 to 1.03 and 0.36 to 1.37, with average value of 0.49 ± 0.16 ($n = 34$) and 0.74 ± 0.34 ($n = 3$). The average values are higher than that of the PAAS (0.01) (Taylor and McLennan, 1985) and lower than that of Black Sea euxinic sediment (4.3) (Calvert and Pedersen, 1993). Only one Ediacaran black shale (ZB-31) displays a higher Mo/Al ratio than 4.3.

Based on the above discussions, it can be inferred that the depositional environment of the Ediacaran and early Cambrian black shales were generally anoxic. Therefore, the influence of the euxinic environment for the positive Eu anomalies could be excluded.

In addition, the Co/Zn ratio may be a sensitive indicator of hydrothermal versus normal authigenic source of trace metals (Toth, 1980). Co/Zn values of the hydrothermal crusts (both manganese-rich and iron-rich) are very low (Co/Zn_{avg} = 0.15), while ferromanganese crust and nodules have an average Co/Zn ratio of 2.5. Both types of black shales have low Co/Zn ratios, averaging 0.29 and 0.22, respectively, which are indicative of a hydrothermal origin for the black shales. Plotting the data of Zn, Co, and Ni concentrations in the Zn-Co-Ni diagram (Jai and Yu, 1992) (Fig. 4), result showed most of the samples are distributed in the field of marine bottom hot-water sediment and none plot in the field of deep ocean manganese nodule of hydrogenetic deposit, which indicate the influences of hydrothermal alteration.

Se tends to be enriched in the mantle and core (Auclair et al., 1987). Compared to the Se concentration of the sea water, hydrothermal vents can provide amount of selenium

Table 5 Statistics values for trace elements and Eu/Eu* values

	Li	Be	Sc	V	Cr	Co	Ni	Cu	Zn	Ga	As	Se	Rb	Sr	Mo	Cd	In	Cs	Ba	Tl	Pb	Bi	Th	U	Eu/Eu*	
C ₁	Maximum	74.15	8.66	32.96	602.0	201.60	20.77	60.69	59.93	32.83	507.03	159.95	5.01	776.79	44.74	17.26	0.89	0.14	22.21	4676.0	2.02	40.82	1.86	21.62	11.05	1.43
	Minimum	14.34	5.03	18.19	86.44	80.97	0.42	5.49	3.49	2.87	208.34	1.96	0.54	394.01	15.91	0.32	0.11	0.07	9.61	1460.0	0.93	0.42	0.27	13.33	2.96	1.07
	Average	28.34	6.77	26.11	269.94	124.70	4.58	28.41	22.62	18.74	367.53	29.11	1.72	618.99	31.51	5.44	0.30	0.11	14.70	3287.77	1.53	9.20	0.76	17.94	6.53	1.25
	SD	15.84	1.19	3.63	166.36	36.96	5.68	17.63	15.90	9.23	116.31	41.44	1.45	124.46	9.30	5.72	0.28	0.02	3.36	1110.37	0.33	12.26	0.52	2.77	2.72	0.12
	Median	23.67	6.80	26.77	258.30	109.20	1.66	28.08	20.03	19.91	398.73	17.77	1.01	652.81	29.96	5.36	0.17	0.12	15.36	3408.0	1.53	6.68	0.54	18.30	5.33	1.29
	EF	1.42	2.26	1.92	2.52	1.50	0.27	0.55	0.84	0.24	21.62	19.41	34.32	5.53	0.09	3.62	3.02	2.22	3.20	5.98	2.04	0.37	5.85	1.68	2.33	
E	Maximum	26.18	9.47	27.66	1795.0	300.10	1.62	36.83	82.33	38.59	504.41	112.84	30.09	888.86	61.12	68.42	0.29	0.23	26.95	4576.0	2.17	60.03	3.99	31.35	9.80	1.44
	Minimum	7.50	2.69	11.77	68.57	93.0	0.39	1.25	0.93	0.15	94.59	0.76	0.25	161.21	14.49	0.11	0.06	0.05	8.12	1087.0	0.64	0.58	0.19	11.32	2.91	0.92
	Average	18.70	7.09	19.82	363.49	149.29	0.83	16.34	26.34	12.16	268.50	21.24	4.84	605.43	23.51	6.96	0.14	0.14	18.56	2508.0	1.58	18.91	0.81	22.30	5.07	1.19
	SD	3.75	1.54	2.95	342.36	42.78	0.29	8.41	23.12	9.10	113.70	26.91	6.28	194.37	8.13	12.20	0.05	0.03	3.78	795.24	0.28	15.46	0.69	4.05	1.53	0.12
	Median	19.12	7.13	19.48	251.90	139.35	0.81	16.89	18.96	11.77	255.23	9.22	2.67	661.64	20.63	2.87	0.14	0.14	17.98	2445.50	1.65	17.91	0.66	22.25	5.09	1.19
	EF	0.93	2.36	1.46	3.40	1.80	0.05	0.37	0.93	0.16	15.79	13.75	9.687	5.41	0.07	4.64	1.48	2.81	4.03	4.56	2.11	0.82	6.22	2.08	1.81	
UCC	Average	20	3	13.6	107	83	17	44	25.0	71	17	1.5	0.05	112	350	1.5	0.1	0.05	4.6	550	0.75	17	0.13	10.7	2.8	
	Median	19.12	7.13	19.48	251.90	139.35	0.81	16.89	18.96	11.77	255.23	9.22	2.67	661.64	20.63	2.87	0.14	0.14	17.98	2445.50	1.65	17.91	0.66	22.25	5.09	1.19

Note: The unit of maximum, minimum, average, SD, and median for trace elements is mg/kg. The data for UCC are according to Taylor and McLennan (1985) and McLennan (2001).

(Auclair et al., 1987), and the Se content is as high as 1640 ppm in the silicate minerals and sulfide assemblages formed under hydrothermal conditions (Roussel et al., 2004). Conversely, Fouquet et al. (1991) found the Se contents of the hydrothermal sediment in the Lau back-arc basin are commonly less than 1.0 ppm. Zhou Yongzhang et al. (1994) reported the hydrothermal origin for the cherts on the top of Lechangxian group in the same area, and the average Se concentration is 3.6 ppm which is 72 times of the UCC. It can be inferred that the hydrothermal fluid at the late Precambrian were enriched in Se. Consequently, the Se in the Ediacaran and early Cambrian black shales were of hydrothermal origin.

4.4.3 Effect of volcanoclastic sources

The Se enrichment is commonly associated with volcanism (Floor and Román-Ross, 2012). All the Ediacaran and early Cambrian black shales fall in the domain of highly-weathered sources in the K₂O-Rb diagram (Fig. 5) (Plank and Langmuir, 1998), which suggests that the volcanic clastic were not the source of high-Se in both the Ediacaran and early Cambrian black shales.

4.4.4 Effect of deep sources

Phosphorus (P) in marine settings is generally derived from one of two provenances (terrestrial sources and upwelling) (Filippelli, 2008). No significant positive correlations are observed between P and Al and Th in the Ediacaran ($r_{P-Al} = -0.18$; $r_{P-Th} = -0.05$) and early Cambrian black shales ($r_{P-Al} = -0.30$; $r_{P-Th} = 0.34$), which indicated that the source of phosphorus in the black shales are upwelling of the deep sea water. In addition, modern mid-ocean ridge environment is generally enriched in Se (Hou Zengqian and Urbae T., 1996). Correlation analysis shows that Se has significant positive correlation with P in the Ediacaran black shales ($r_{Se-P} = 0.41$, $P < 0.05$), while no significant positive correlation between Se and P ($r_{Se-P} = 0.27$) is observed in the early Cambrian black shales. Thus, P sources in the Ediacaran black shales were likely related to the upwelling of the deep seawater, which may simultaneously bring abundant Se sources from the deep water. On the other hand, the Se concentrations in the early Cambrian black shales are not related to the upwelling of the deep seawater.

4.4.5 Contribution of the pyrite

Cluster analysis is widely used in the geological study (Dai et al., 2005; Dai Mingjian et al., 2015). Cluster analysis displays that Se in the Ediacaran black shales are associated with Bi, Fe, P, Ni, and As (Fig. 6a), and Se, Fe, Sc, Tl, Ti and Cr are associated together in the early

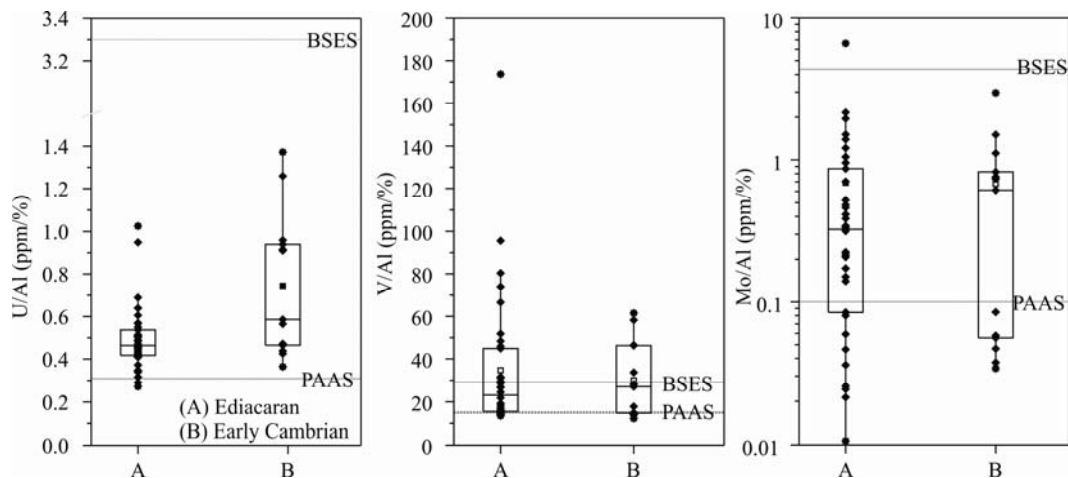


Fig. 3. Box plots (Lucja et al., 2015) of U/Al, V/Al, and Mo/Al ratios (ppm%) of the Ediacaran and early Cambrian black shales, in the Guangning area, western Guangdong Province, South China. BSES is short for Black Sea euxinic sediment.

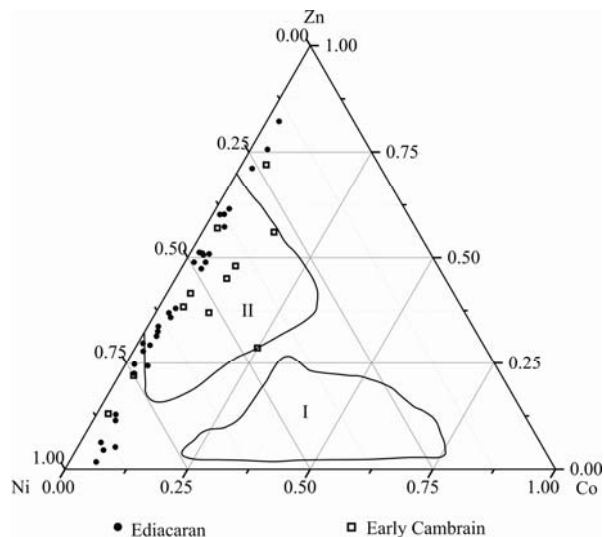


Fig. 4. Zn-Co-Ni triangular diagram of the Ediacaran and early Cambrian black shales in the Guangning area, western Guangdong Province, South China, according to Jai and Yu (1992).

I, Deep ocean manganese nodule of hydrogenetic deposit; II, Marine bottom hot-water sediment.

Cambrian black shales (Fig. 6b). Additionally, Fe contents in the Ediacaran black shales show significant positive correlation with S ($r_{Fe-S} = 0.52$, $P < 0.01$), which is an indicator of the presence of pyrite. However, there is no significant positive correlation between Fe and S ($r = 0.45$) in the early Cambrian black shales. Thus, the presence of pyrite in the Ediacaran black shales may explain their Se-rich nature (Zhang Aiyun et al., 1987).

5 Conclusions

Detailed analyses of major and trace elements concentrations were conducted for the Ediacaran and early Cambrian black shales in the Guangning area, western

Guangdong Province, south China. Our results are briefly summarized below:

(1) Compared with the UCC, the Ediacaran black shales are strongly enriched in Se, Ga, significantly enriched in As, Bi and Rb, weakly enriched in Mo, Ba, Cs, V, In, Be, Tl, and Th, normal in U, Cr, Cd, Sc, Pb, Cu, and Li, and depleted in Ni, Zn, Sr, and Co. Early Cambrian black shales display strongly enriched Se, Ga, and As, significantly enriched Ba, Bi, and Rb, weakly enriched Mo, Cs, Cd, V, U, Be, In, and Tl, normal Sc, Th, Cr, Li, Cu, Ni, and Pb and depleted Co, Zn, and Sr.

(2) Similar with the Se-rich Ediacaran and early Cambrian black shales in the Yangtze block, the Ediacaran and early Cambrian black shales in this study area in the Cathaysia block are also enriched in Se. Moreover, Se is the most enriched trace element among the 24 trace elements. In the Ediacaran and early Cambrian black

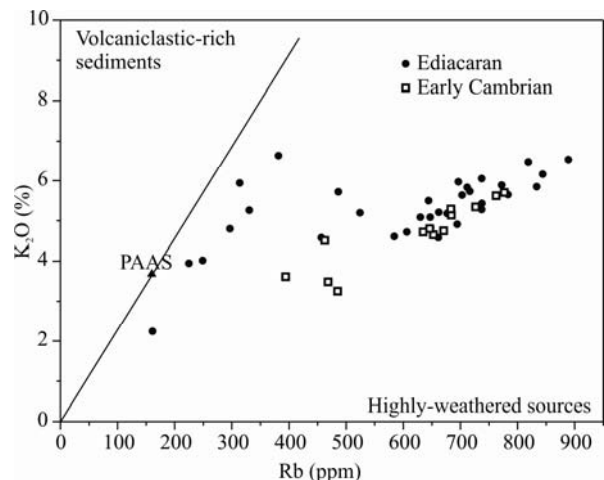


Fig. 5. K₂O-Rb diagram (according to Plank and Langmuir, 1998) of the Ediacaran and early Cambrian black shales, in the Guangning area, western Guangdong Province, South China.

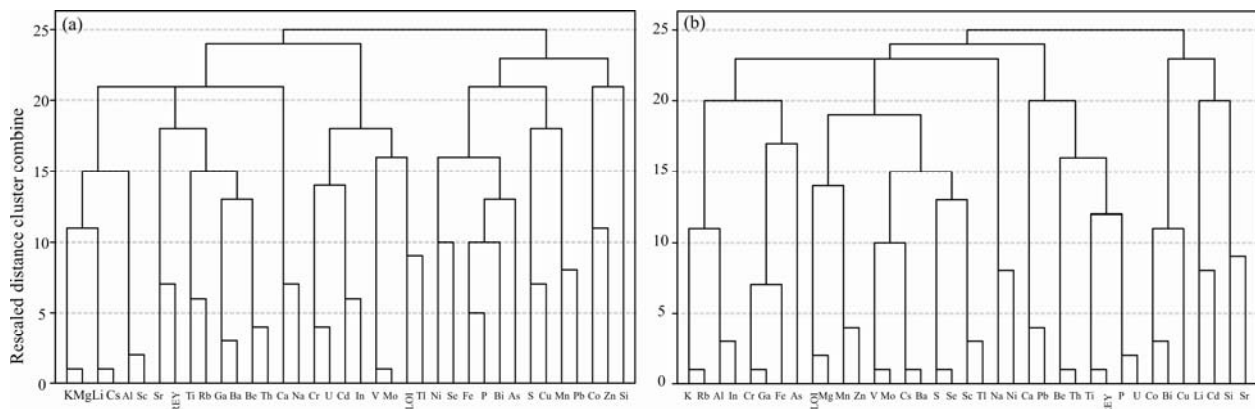


Fig. 6. Dendrogram produced by hierarchical cluster analysis of analytical data from Ediacaran (a) and early Cambrian (b) black shale samples in the Guangning area (cluster method, centroid clustering, Pearson correlation).

shales, Se concentrations vary from 0.25 to 30.09 ppm and 0.54 to 5.01 ppm, have average values of 4.84 and 1.72 ppm, and average EF values of 96.87 and 34.32 relative to UCC, respectively. The maximum Se concentration occurs in the Ediacaran black shales, and the average content of Se in the Ediacaran black shales is 2.8 times higher than that of early Cambrian black shales.

(3) Variance analysis suggests that Se concentrations in the Ediacaran and early Cambrian black shales exhibit significant difference ($P = 0.03$). Provenance analysis shows that Se contents of both the Ediacaran and early Cambrian black shales were without detrital provenance and volcaniclastic sources, but may have a hydrothermal origin. The deep sources and the presence of pyrite may explain the higher Se contents in the Ediacaran black shales.

Acknowledgments

This research was supported by the National Natural Science Foundation of China (Grant No. 41172310, 41472322 and 40872210), the National Basic Research Program of China (Grant No. 2014CB238906), the Local Science and Technology Tasks “Distribution Patterns and Prospect of Exploitation and Utilization of Selenium in Foshan area, Guangdong” and “Construction for Laboratory of Selenium Resources Comprehensive Utilization”. We thank Mr. Chen Weiqiang, Han Jiucheng and Du Yajun for help in the field, and Dr. Wang Shaobin for his informative advice.

Manuscript received Feb. 3, 2016
accepted July 20, 2016
edited by Fei Hongcui

References

- Algeo, T.J., and Lyons, T.W., 2006. Mo–total organic carbon covariation in modern anoxic marine environments: Implications for analysis of paleoredox and paleohydrographic conditions. *Paleoceanography*, 21.
- Algeo, T.J., and Maynard, J.B., 2004. Trace-element behavior and redox facies in core shales of Upper Pennsylvanian Kansas-type cyclothems. *Chemical Geology*, 206: 289–318.
- Auclair, G., Fouquet, Y., and Bohn, M., 1987. Distribution of selenium in high-temperature hydrothermal sulfide deposits at 13°N, East Pacific Rise. *Canadian Mineralogist*, 25: 577–587.
- Bau, M., and Dulski, P., 1996. Distribution of yttrium and rare-earth elements in the Penge and Kuruman iron-formations, Transvaal Supergroup, South Africa. *Precambrian Research*, 79: 37–55.
- BGMRGD (Bureau of Geology and Mineral Resources of Guangdong Province), 1988. *Regional Geology of Guangdong Province*. Geological Publishing House, Beijing (in Chinese).
- Brookins, D., 1989. Aqueous geochemistry of rare earth elements. *Reviews in Mineralogy and Geochemistry*, 21: 201–225.
- Calvert, S., and Pedersen, T., 1993. Geochemistry of recent oxic and anoxic marine sediments: implications for the geological record. *Marine geology*, 113: 67–88.
- Chen Xi, Ling Hongfei, Vance, D., Shields-Zhou, G.A., Zhu Maoyan, Poulton, S.W., Och, L.M., Jiang Shaoyong, Li Da, Cremonese, L., and Archer, C., 2015. Rise to modern levels of ocean oxygenation coincided with the Cambrian radiation of animals. *Nature Communication*, 6.
- Cheng Lixue, Wang Yuanjun, Chen Hongde, Wang Yue and Zhong Yijiang, 2013. Sedimentary and burial environment of black shales of Sinian to Early Palaeozoic in Upper Yangtze region. *Acta Petrologica Sinica*, 29(8): 2906–2912 (in Chinese with English abstract).
- Condon, D., Zhu Maoyan, Bowring, S., Wang Wei, Yang Aihua and Jin Yugan, 2005. U-Pb Ages from the Neoproterozoic Doushantuo Formation, China. *Science*, 308: 95–98.
- Conway, M.S., 2000. The Cambrian “explosion”: Slow-fuse or megatonnage? *Proceedings of the National Academy of Sciences of the United States of America*, 97: 4426–4429.
- Dai Mingjian, Liu Lu, Lee Dongjin, Peng Yunbiao and Miao Aisheng, 2015. Morphometrics of heliolites (Tabulata) from the Late Ordovician, Yushan, Jiangxi, South China. *Acta Geologica Sinica* (English Edition), 89(1): 38–54.
- Dai Shifeng, Ren Deyi, Tang Yuegang, Yue Ming and Hao Liming, 2005. Concentration and distribution of elements in Late Permian coals from western Guizhou Province, China. *International Journal of Coal Geology*, 61: 119–137.

- Derry, L.A., and Jacobsen, S.B., 1990. The chemical evolution of Precambrian seawater: Evidence from REEs in banded iron formations. *Geochimica et Cosmochimica Acta*, 54: 2965–2977.
- Fan Delian, Yang Xiuzhen, Wang Lianfang and Chen Nansheng, 1973. Petrological and geochemical characteristics of a nickel-molybdenum-multielement-bearing lower-Cambrian black shale from a certain district in South China. *Geochimica*, 3: 143–164 (in Chinese with English abstract).
- Fan Haifeng, Wen Hanjie, Hu Ruizhong and Zhao Hui, 2011. Selenium speciation in Lower Cambrian Se-enriched strata in South China and its geological implications. *Geochimica et Cosmochimica Acta*, 75: 7725–7740.
- Feng Caixia, Chi Guoxiang, Liu Jiajun, Hu Ruizhong, Liu Shen and Coulson, I.M., 2012. Geochemical constraints on the origin and environment of Lower Cambrian, selenium-rich siliceous sedimentary rocks in the Ziyang area, Daba region, central China. *International Geology Review*, 54: 765–778.
- Feng Caixia, Liu Jiajun, Hu Ruizhong and Liu Shen, 2004. Geochemistry of the Yutangba Se deposit in western Hubei, China. *Chinese Journal of Geochemistry*, 23: 255–264.
- Fike, A.D., Grotzinger, J.P., Pratt, L.M., and Summons, R.E., 2006. Oxidation of the Ediacaran Ocean. *Nature*, 444: 744–747.
- Filippelli, G.M., 2008. The global phosphorus cycle: past, present, and future. *Elements*, 4: 89–95.
- Floor, G.H., and Román-Ross, G., 2012. Selenium in volcanic environments: a review. *Applied Geochemistry*, 27: 517–531.
- Fouquet, Y., Stackelberg, U., Charlou, J.L., Donval, J.P., Foucher, J.P., Erzinger, J., Herzog, P., Mühe, R., Wiedicke, M., Soakai, S., and Whitechurch, H., 1991. Hydrothermal activity in the Lau back-arc basin: Sulfides and water chemistry. *Geology*, 19: 303–306.
- Guo Qingjun, Shields, G.A., Liu Congqiang, Strauss, H., Zhu Maoyan, Pi Daohui, Goldberg, T., and Yang Xinglian, 2007. Trace element chemostratigraphy of two Ediacaran–Cambrian successions in South China: Implications for organosedimentary metal enrichment and silicification in the Early Cambrian. *Palaeogeography, Palaeoclimatology, Palaeoecology*, 254: 194–216.
- Helz, G.R., Miller, C.V., Charnock, J.M., Mosselmans, J.F.W., Patrick, R.A.D., Garner, C.D., and Vaughan, D.J., 1996. Mechanism of molybdenum removal from the sea and its concentration in black shales: EXAFS evidence. *Geochimica et Cosmochimica Acta*, 60: 3631–3642.
- Hou Zengqian and Urabe, T., 1996. A comparative study on geochemistry of sulfide ores from the kuroko-type deposits on ancient and modern sea-floor. *Geochimica*, 25(3): 228–241 (in Chinese with English abstract).
- Jai, H.C., and Yu, H., 1992. Geochemistry and depositional environment of Mn oxide deposits in the Tokoro Belt, northeastern Hokkaido, Japan. *Economic Geology*, 87: 1265–1274.
- Kamber, B.S., and Webb, G.E., 2001. The geochemistry of late Archaean microbial carbonate: implications for ocean chemistry and continental erosion history. *Geochimica et Cosmochimica Acta*, 65: 2509–2525.
- Knoll, A.H., and Carroll, S.B., 1999. Early animal evolution: emerging views from comparative biology and geology. *Science*, 284: 2129–2137.
- Knoll, A.H., Walter, M.R., Narbonne, G.M., and Christie-Blick, N., 2004. A new period for the geologic time scale. *Science*, 305: 621–622.
- Krye, K.A., Murray, R.W., and Murray, D.W., 2003. Al-to-oxide and Ti-to-organic linkages in biogenic sediment: relationships to paleo-export production and bulk Al/Ti. *Earth and Planetary Science Letters*, 211: 125–141.
- Li Renwei, Lu Jialan, Zhang Shukun and Lei Jiajin, 1999. Organic carbon isotopic composition of the sinian and early Cambrian black shales. *Science in China Series D: Earth Sciences*, 29(4): 351–357 (in Chinese).
- Li Shuangying, 1994. Concentration and enrichment mechanism of Se of Lantian formation (LF), upper Sinian in South Anhui. *Journal of Hefei University of Technology (Natural Science)*, 17, 203–209 (in Chinese with English abstract).
- Li Xianhua, Li Zhengxiang and Li Wuxian, 2014. Detrital zircon U–Pb age and Hf isotope constrains on the generation and reworking of Precambrian continental crust in the Cathaysia Block, South China: A synthesis. *Gondwana Research*, 25: 1202–1215.
- Li Zhengxiang, Bogdanova, S.V., Collins, A.S., Davidson, A., De Waele, B., Ernst, R.E., Fitzsimons, I.C.W., Fuck, R.A., Gladkochub, D.P., Jacobs, J., Karlstrom, K.E., Lu, S., Natapov, L.M., Pease, V., Pisarevsky, S.A., Thrane, K., and Vernikovsky, V., 2008. Assembly, configuration, and break-up history of Rodinia: A synthesis. *Precambrian Research*, 160: 179–210.
- Lucia, F.F., Li Chuankui, Li Qian, Meng Jin and Wang Yuanqing, 2015. Strenulagus (Mammalia: Lagomorpha) from the Middle Eocene Irdin Manha Formation of the Erlan Basin, Nei Mongol, China. *Acta Geologica Sinica (English Edition)*, 89 (1): 12–26.
- Luo Kunli, 2011. Arsenic and fluorine contents and distribution patterns of early Paleozoic stonelike coal in the Daba fold zone and Yangtze Plate, China. *Energy & Fuels*, 25: 4479–4487.
- Luo Kunli, Xu Lirong, Tan Jianan, Wang Duohu and Xiang Lianhua, 2004. Selenium source in the selenosis area of the Daba region, South Qinling Mountain, China. *Environmental Geology*, 45: 426–432.
- Lyons, T.W., Anbar, A.D., Severmann, S., Scott, C., and Gill, B.C., 2009. Tracking euxinia in the ancient ocean: a multiproxy perspective and Proterozoic case study. *Annual Review of Earth and Planetary Sciences*, 37: 507–534.
- Ma Lifang, 2002. Geological atlas of China. Geological Publishing House, Beijing (in Chinese).
- McLennan, S.M., 2001. Relationships between the trace element composition of sedimentary rocks and upper continental crust. *Geochemistry, Geophysics, Geosystems*, 2: 1021.
- Michard, A., and Albarède, F., 1986. The REE content of some hydrothermal fluids. *Chemical Geology*, 55: 51–60.
- Nance, W.B., and Taylor, S.R., 1976. Rare-earth element patterns and crustal evolution I: Australian post-Archean sedimentary rocks. *Geochimica et Cosmochimica Acta*, 40: 1539–1551.
- Ni Runxiang, Luo Kunli, Tian Xinglei, Yan Songgui, Zhong Jitai and Liu Maoqiu, 2015. Distribution and geological sources of selenium in environmental materials in Taoyuan County, Hunan Province, China. *Environmental Geochemistry and Health*, 1–12.
- Olivarez, A.M., and Owen, R.M., 1991. The europium anomaly of seawater: implications for fluvial versus hydrothermal REE inputs to the oceans. *Chemical Geology*, 92: 317–328.

- Peng Shaomei, He Shaoxun and Duan Jiarui, 1991. Distribution characteristics of gold and other microelements in the Sinian Lechangxia Group in Qingyuan-Yingde area, Guangdong Province. *Journal of Central South University*, 22(6): 597–607 (in Chinese with English abstract).
- Pi Daohui, Liu Congqiang, Shields-Zhou, G.A., and Jiang Shaoyong, 2013. Trace and rare earth element geochemistry of black shale and kerogen in the early Cambrian Niutitang Formation in Guizhou province, South China: Constraints for redox environments and origin of metal enrichments. *Precambrian Research*, 225: 218–229.
- Plank, T., and Langmuir, C.H., 1998. The chemical composition of subducting sediment and its consequences for the crust and mantle. *Chemical geology*, 145: 325–394.
- Qiu Zhihua, Zhong Zhicheng and Li Jinhong, 2011. Analysis of climate comfort degree for tourism in Guangning Country. *Guangdong Meteorology*, 33(6): 54–55 (in Chinese).
- Rouxel, O., Fouquet, Y., and Ludden, J.N., 2004. Subsurface processes at the lucky strike hydrothermal field, Mid-Atlantic ridge: evidence from sulfur, selenium, and iron isotopes 1. *Geochimica et Cosmochimica Acta*, 68: 2295–2311.
- Sahoo, S.K., Planavsky, N.J., Kendall, B., Wang Xinjiang, Shi Xiaoying, Scott, C., Anbar, A.D., Lyons, T.W., and Jiang Ganqing, 2012. Ocean oxygenation in the wake of the Marinoan glaciation. *Nature*, 489: 546–549.
- Schröder, S., and Grotzinger, J.P., 2007. Evidence for anoxia at the Ediacaran–Cambrian boundary: the record of redox-sensitive trace elements and rare earth elements in Oman. *Journal of the Geological Society*, 164: 175–187.
- Scott, C., Lyons, T.W., Bekker, A., Shen Yanan, Poulton, S.W., Chu Xuelei and Anbar, A.D., 2008. Tracing the stepwise oxygenation of the Proterozoic ocean. *Nature*, 452: 456–459.
- Steiner, M., Wallis, E., Erdtmann, B.D., Zhao Yuanlong and Yang Ruidong, 2001. Submarine-hydrothermal exhalative ore layers in black shales from South China and associated fossils — insights into a Lower Cambrian facies and bio-evolution. *Palaeogeography, Palaeoclimatology, Palaeoecology*, 169: 165–191.
- Shen Shuzhong, Zhu Maoyan, Wang Xiangdong, Li Guoxiang, Cao Changqun and Zhang Hua, 2010. A comparison of the biological, geological events and environmental backgrounds between the Neoproterozoic-Cambrian and Permian-Triassic transitions. *Science China Earth Science*, 53: 1873–1884.
- Sverjensky, D.A., 1984. Europium redox equilibria in aqueous solution. *Earth and Planetary Science Letters*, 67: 70–78.
- Taylor, S.R., and McLennan, S.M., 1985. The continental crust: its composition and evolution. Blackwell, Malden, Mass.
- Tian Xinglei and Luo Kunli, 2017a. Distribution and enrichment patterns of selenium in the Ediacaran and early Cambrian strata in the Yangtze Gorges area, South China. *Science China Earth Sciences*, 60: 1268–1282.
- Tian Xinglei and Luo Kunli, 2017b. Selenium, arsenic and molybdenum variation and bio-radiation in the Ediacaran–Cambrian interval. *Precambrian Research*, 292: 378–385.
- Toth, J.R., 1980. Deposition of submarine crusts rich in manganese and iron. *Geological Society of America Bulletin*, 91: 44–54.
- Tribouillard, N., Algeo, T.J., Lyons, T., and Riboulleau, A., 2006. Trace metals as paleoredox and paleoproductivity proxies: An update. *Chemical Geology*, 232: 12–32.
- Wang Libo, Jiu Kai, Zeng Weite and Fu Jinglong, 2013. Characteristics of Lower Cambrian marine black shales and evaluation of shale gas prospective area in Qianbei area, Upper Yangtze region. *Acta Petrologica Sinica*, 29(9): 3263–3278 (in Chinese with English abstract).
- Wen Hanjie and Qiu Yuzhuo, 2002. Geology and Geochemistry of Se-Bearing Formations in Central China. *International Geology Review*, 44: 164–178.
- Wu Chaodong, Zeng Fanggang, Lei Jiajin and Zhao Rui, 1999. Referential significance of sulfur isotopes and separation of S species in black shales of Southwest China. *Chinese science bulletin*, 44: 1612–1616 (in Chinese).
- Xia Wei, Yu Bingsong and Sun Mengdi, 2015. Depositional settings and enrichment mechanism of organic matter of the black shales at the bottom of Niutitang Formation, Lower Cambrian in Southeast Chongqing: A case study from Well Yuke 1. *Acta Geologica Sinica* (English Edition), 89(S1): 287–287.
- Yu Lingang, Lehmann, B., Zhang Xigui, Zheng Wei and Meng Qingtian, 2014. Trace element distribution in black shales from the Kunyang phosphorite deposit and its geological significances. *Acta Petrologica Sinica*, 30(6): 1817–1827 (in Chinese with English abstract).
- Zhang Aiyun, Wu Damao, Guo Lina and Wang Yunlong, 1987. Geochemistry of marine black shale formation and its metallogenetic significance. Science Press (Beijing).
- Zhang Qiuying, 2000. Uraniferous black shale and related uranium mineralization features in South China. *Acta Geologica Sinica* (English Edition), 74(3): 602–604.
- Zhang Xingliang and Shu Degan, 2014. Causes and consequences of the Cambrian explosion. *Science China: Earth Science*, 57: 930–942.
- Zhang Zhilan, Yuan Haihua, Ling Jingsheng and Chen Taiping, 1992. Preliminary study on isotopic geochronology of Lechangxia Group in Gushui, Guangning Country. *Guangdong Geology*, 7(1): 51–59 (in Chinese with English abstract).
- Zhao Guochun and Cawood, P.A., 2012. Precambrian geology of China. *Precambrian Research*, 222–223: 13–54.
- Zhou Yongzhang, Tu Guangzhi, Chown, E.H., Guha, J., and Lu Huanzhang, 1994. Petrologic and geochemical characteristics and origin of Gushui cherts, Guangdong Province, China. *Chinese Journal of Geochemistry*, 13(2): 118–131.
- Zhuang Hanping, Lu Jialan, Fu Jiamo, Liu Jinzhong, Ren Chigang, Zou Degang and Tian Weizhi, 1998. Organic/inorganic occurrence of metallic elements of the black shale-hosted Baiguoyuan Silver-Vanadium deposit in Xingshan, Hubei. *Acta Geologica Sinica* (English Edition), 72(2): 299–307.

About the first author

TIAN Xinglei: Male, born in 1987 in Qingzhou City, Shandong Province; Ph. D, graduated from the Institute of Geographic Sciences and Natural Resources Research, University of Chinese Academy of Sciences; Now He is a postdoctoral fellow in Shandong Institute of Geological Sciences. His research interests are the distribution and enrichment patterns of biological trace element in the strata and paleowater and their biological response during the crucial periods of biological evolution. Email: xinglei_tian@163.com.